

EFFECT OF Na DOPING ON SOME PHYSICAL PROPERTIES OF CHEMICALLY SPRAYED CZTS THIN FILMS[†]

 Noura J. Mahdi,  Nabeel A. Bakr*

Department of Physics, College of Science, University of Diyala, Diyala, Iraq

**Corresponding Author: nabeelalibakr@yahoo.com*

Received August 3, 2022; revised August 18, 2022; accepted August 25, 2022

In this work, sodium-doped copper zinc tin sulfide (CZTS) thin films are prepared by depositing them on glass substrates at temperature of (400 ± 10) °C and thickness of (350 ± 10) nm using Chemical Spray Pyrolysis (CSP) technique. 0.02 M of copper chloride dihydrate ($\text{CuCl}_2 \cdot 2\text{H}_2\text{O}$), 0.01 M of zinc chloride (ZnCl_2), 0.01 M of tin chloride dihydrate ($\text{SnCl}_2 \cdot 2\text{H}_2\text{O}$), and 0.16 M of thiourea ($\text{SC}(\text{NH}_2)_2$) were used as sources of copper, zinc, tin, and sulphur ions respectively. Sodium chloride (NaCl) at different volumetric ratios of (1, 3, 5, 7 and 9) % was used as a dopant source. The solution is sprayed on glass substrates. XRD diffraction, Raman spectroscopy, FESEM, UV-Vis-NIR, and Hall effect techniques were used to investigate the structural, optical, and electrical properties of the produced films. The XRD diffraction results revealed that all films are polycrystalline, with a tetragonal structure and a preferential orientation along the (112) plane. The crystallite size of all films was estimated using Scherrer's method, and it was found that the crystallite size decreases as the doping ratio increases. The FESEM results revealed the existence of cauliflower-shaped nanoparticles. The optical energy band gap was demonstrated to have a value ranging from 1.6 to 1.51 eV with a high absorption coefficient ($\alpha \geq 10^4 \text{ cm}^{-1}$) in the visible region of the spectrum. Hall measurements showed that the conductivity of CZTS thin films with various Na doping ratios have p-type electrical conductivity, and it increases as the Na doping ratio increases.

Keywords: CZTS thin films, Na doping, Structural properties, Optical properties, Hall effect.

PACS: 88.40.jn; 73.61.-r; 81.15.Rs; 61.82.Fk; 78.20.-e

$\text{Cu}_2\text{ZnSnS}_4$ has been considered an alternative to the well-known $\text{Cu}(\text{In,Ga})\text{Se}_2$ (CIGS) materials for several years because it is a quaternary semiconductor made up of non-toxic and earth abundant minerals. It is manufactured by replacing the In/Ga in the CIGS system with Zn/Sn, making it a potential candidate for optoelectronic applications. Despite similarities in crystal structure, absorption coefficient, optical band gap E_g , and device architecture between (CZTS) quaternary compound and (CIGS) system, CZTS-based solar cells have a record efficiency of 12.6 %, which is significantly lower than that of CIGS (22.6 %) [1, 2]. Sodium-doped thin films extend the life of defects by passivating them, which has an impact on chemical composition by lowering ZnS development due to Sn loss inhibition [3]. Due to its photoelectric features, such as high absorption coefficient, P type carrier, abundance of its constituents, and absence of component toxicity, the quaternary $\text{Cu}_2\text{ZnSnS}_4$ combination is a potential material for low-cost absorption bands in solar cell applications [4, 5]. The efficiency of solar cells has been low in comparison to $\text{Cu}(\text{In,Ga})\text{Se}_2$ so far, and this is due to defects and secondary stages [6,7]. Chemical spray pyrolysis has attracted many researchers because it contributes to the preparation of many thin-film materials at a low cost compared to other techniques that require high-cost and complex devices, as well as the fact that it does not require substrates or targets with high quality [8, 9]. The aim of this study is to deposit thin films of CZTS doped with sodium with various concentrations in order to enhance the properties of the CZTS thin films and to compare the experimental results with those of previous studies to better understand the effect of doping on the structural and optical properties of CZTS films.

EXPERIMENTAL PROCEDURE

Chemical spray pyrolysis was used to deposit $\text{Cu}_2\text{ZnSnS}_4$ (CZTS) thin films on soda-lime glass substrates at a temperature of 400 ± 10 °C and a thickness of 350 ± 10 nm. The glass substrates are cleaned with ultrasonic waves in distilled water, acetone, and distilled water for a period of no more than 10 minutes, and then dried with soft paper. The spray solution is prepared by dissolving 0.02 M of copper chloride dihydrate ($\text{CuCl}_2 \cdot 2\text{H}_2\text{O}$), 0.01 M of zinc chloride (ZnCl_2), 0.01 M of tin chloride dihydrate ($\text{SnCl}_2 \cdot 2\text{H}_2\text{O}$), and 0.16 M of thiourea ($\text{SC}(\text{NH}_2)_2$) in distilled water. Each powder is dissolved separately in a volume of (25 ml) of distilled water, and filtered separately before being mixed together to get the final solution used to prepare the undoped films (CZTS). The doping solution of 0.1 M concentration was made by dissolving 0.5844 g of NaCl in 100 ml of distilled water. This solution is added to the quaternary solution at a volumetric ratios of (1, 3, 5, 7, and 9) % as shown in Table 1. The final solution is mixed for 15 minutes with a magnetic stirrer until a clear homogenous solution is obtained. For weighing powders, an electronic balance (Mettler AE-160 type) with a sensitivity of 10^{-4} g was used. The spraying process is carried out for a period of 10 seconds and to prevent the substrate from losing its heat, the process is paused for 2 minutes. The process is repeated until the desired thickness of the films is achieved. The resulting films are stable with good adhesion and having thickness of 350 ± 10 nm.

[†] Cite as: N.J. Mahdi, and N.A. Bakr, East Eur. J. Phys. 3, 84 (2022), <https://doi.org/10.26565/2312-4334-2022-3-11>

© N.J. Mahdi, N.A. Bakr, 2022

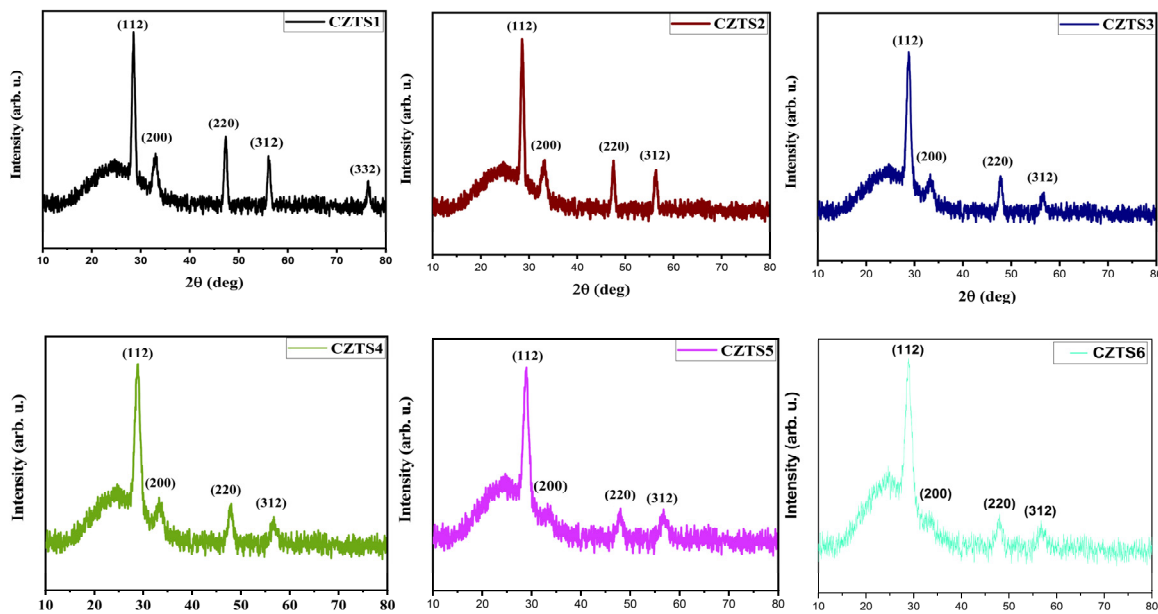
Table 1. Volumetric doping ratios of sodium chloride used in CZTS thin films preparation.

Sample	Volumetric Doping Ratio %
CZTS1	0 (undoped)
CZTS2	1
CZTS3	3
CZTS4	5
CZTS5	7
CZTS6	9

RESULTS AND DISCUSSION

XRD analysis

Figure 1 shows the X-ray diffraction patterns of Na-doped CZTS films. The figure reveals peaks located at $2\theta \sim 28.53^\circ, 33.24^\circ, 47.56^\circ$ and 56.36° , assigned to the planes (112), (200), (220) and (312) of CZTS kesterite structure respectively based on (ICDD) card number (26-0575) and this is in agreement with the results of previous studies [10-12].

**Figure 1.** X-ray diffraction patterns of Na-doped CZTS thin films at different doping ratios

The peak appeared at $2\theta \sim 76.5^\circ$ in the XRD pattern of the undoped sample (CZTS1) is assigned to (332) plane and it disappears in the patterns of all doped samples. The X-ray diffraction patterns revealed that the films have multiple diffraction peaks, indicating that the films are polycrystalline with a tetragonal crystal structure, with the preferred growth direction (112) occurring at $2\theta \sim 28.5^\circ$, which is consistent with previous studies [10,11]. From tetragonal structure the interplanar spacing (d) is given by [13]:

$$\frac{1}{d^2} = \left(\frac{h^2 + k^2}{a^2} \right) + \frac{1}{c^2}, \quad (1)$$

Where h, k and l are the Miller indices and a, b and c are lattice constants of the tetragonal unit cell. The lattice constants were estimated and presented in the table (2). It can be seen that the extracted results are close to the standard values of the lattice constants $a = b = 5.42 \text{ \AA}$ and $c = 10.84 \text{ \AA}$. The lattice vector ($c/2a$) ratio in the ideal tetragonal configuration is 1, and it can be seen that this ratio of all samples is very close to the ideal one. The crystallite size of the Na-doped CZTS thin films is determined by using the Scherrer's formula shown below [14]:

$$D = K\lambda/\beta\cos\theta, \quad (2)$$

where K is the Scherrer's constant, λ is the wavelength of the X-rays incident on the target with a value of (1.54056 \AA), β is the full-width at half maximum (FWHM) in radians and θ is the Bragg angle.

The resulting values for the crystallite size are shown in the Table 2. The maximum value of the crystals size is 12 nm belongs to the CZTS1 sample, and we can conclude that the increase in the Na-doping ratio affects the crystallinity of the grown films. It is possible to summarize what happens to metal ions when Na is introduced into the CZTS host network. Lattice distortion occurs due to the difference in the diameter of the ions and the arrangement of the valence electron, and thus the results show that the distortion in the lattice of the samples was small [15].

Table 2. Structural parameters of the XRD results of Na-doped CZTS thin films at different doping ratios.

Sample	2 θ (deg.) (112)	d (Å)	FWHM (deg.) (112)	D (nm)	Lattice constants (Å)		c/2a	Unit cell volume (Å ³)
					a = b	c		
CZTS1	28.53	3.129	0.6829	12.00	5.432	10.798	0.994	318.613
CZTS2	28.61	3.114	0.7064	11.61	5.431	10.862	1.000	320.383
CZTS3	28.80	3.107	1.0125	8.10	5.440	10.962	1.008	324.405
CZTS4	28.85	3.107	1.2951	6.33	5.408	10.863	1.004	317.704
CZTS5	28.90	3.112	1.2951	6.33	5.407	10.950	1.013	320.130
CZTS6	28.95	3.112	1.3000	6.31	5.410	10.994	1.016	321.773

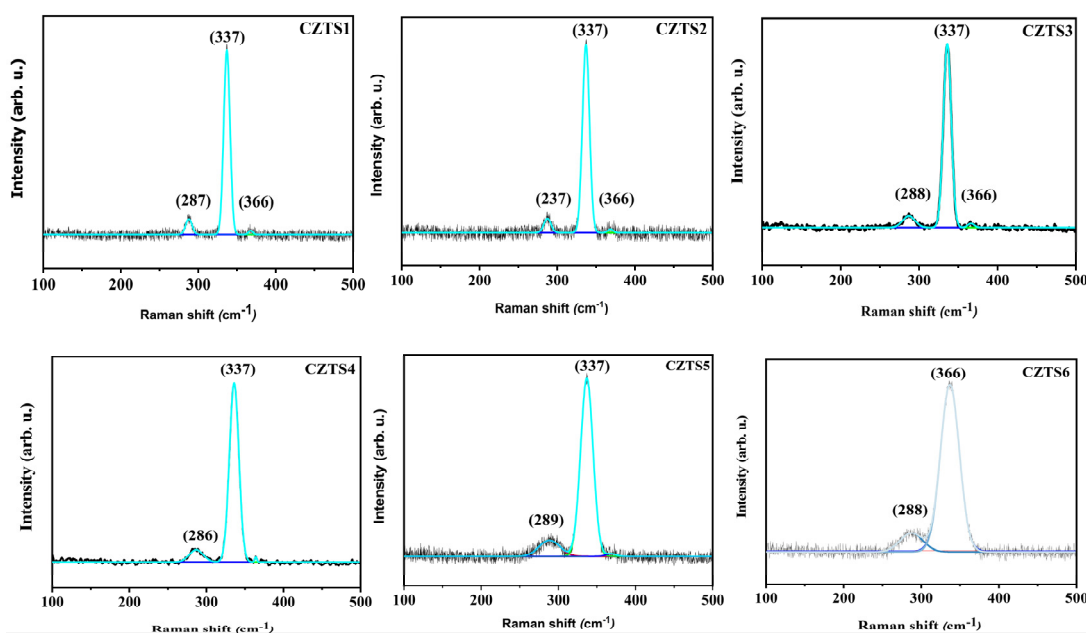
Raman spectroscopy analysis

Raman spectroscopy is widely used to determine the presence of secondary phases in materials. In addition to the presence of other less intense peaks that occur in the locations indicated in Table 3, the Raman spectra revealed that the samples' main peak is located at ~ 337 cm^{-1} , which has been attributed to the kesterite CZTS, and this is in agreement with the conclusions of previous studies [11, 12].

Table 3. Results of Raman spectroscopy of Na-doped CZTS thin films at different doping ratios.

Sample	Peak center (cm^{-1})	Peak width (cm^{-1})	Intensity (arb. u.)
CZTS1	287	8.15	7.50
	237	8.04	69.65
	366	5.55	3.01
CZTS2	287	9.14	10.41
	337	9.09	69.52
	366	6.55	7.61
CZTS3	288	15.79	5.81
	337	10.07	60.3
	366	8.17	3.18
CZTS4	286	17.99	5.68
	337	12.11	59.15
CZTS5	289	26.6	7.32
	337	16.17	59.27
CZTS6	288	28.33	8.06
	336	24.30	57.01

Raman spectra of thin Na-doped CZTS films at different doping ratios are shown in Figure 2. Strain, phonon confinement, defects, and nonstoichiometry of the size distribution are just a few of the factors that might influence the position of the Raman peak [16]. The variation in Raman intensity is caused by the high frequency dielectric constant changing [17].

**Figure 2.** Raman spectra of Na-doped CZTS thin films at different doping ratios

Field Emission Scanning Electron Microscopy (FESEM) measurements

Figure 3 shows the FESEM micrographs (of 50 KX magnification) of the Na-doped CZTS thin films deposited in the present study. It can be seen that the surface structure of the films has a cauliflower-like shapes in the nano-scale with irregular particle size and distribution where the granular boundaries are clear. Also, there are a number of voids and cracks resulting from crystal defects and secondary growth on the surface. It can be concluded that a new layer starts to grow before the growth completion of the beneath layer.

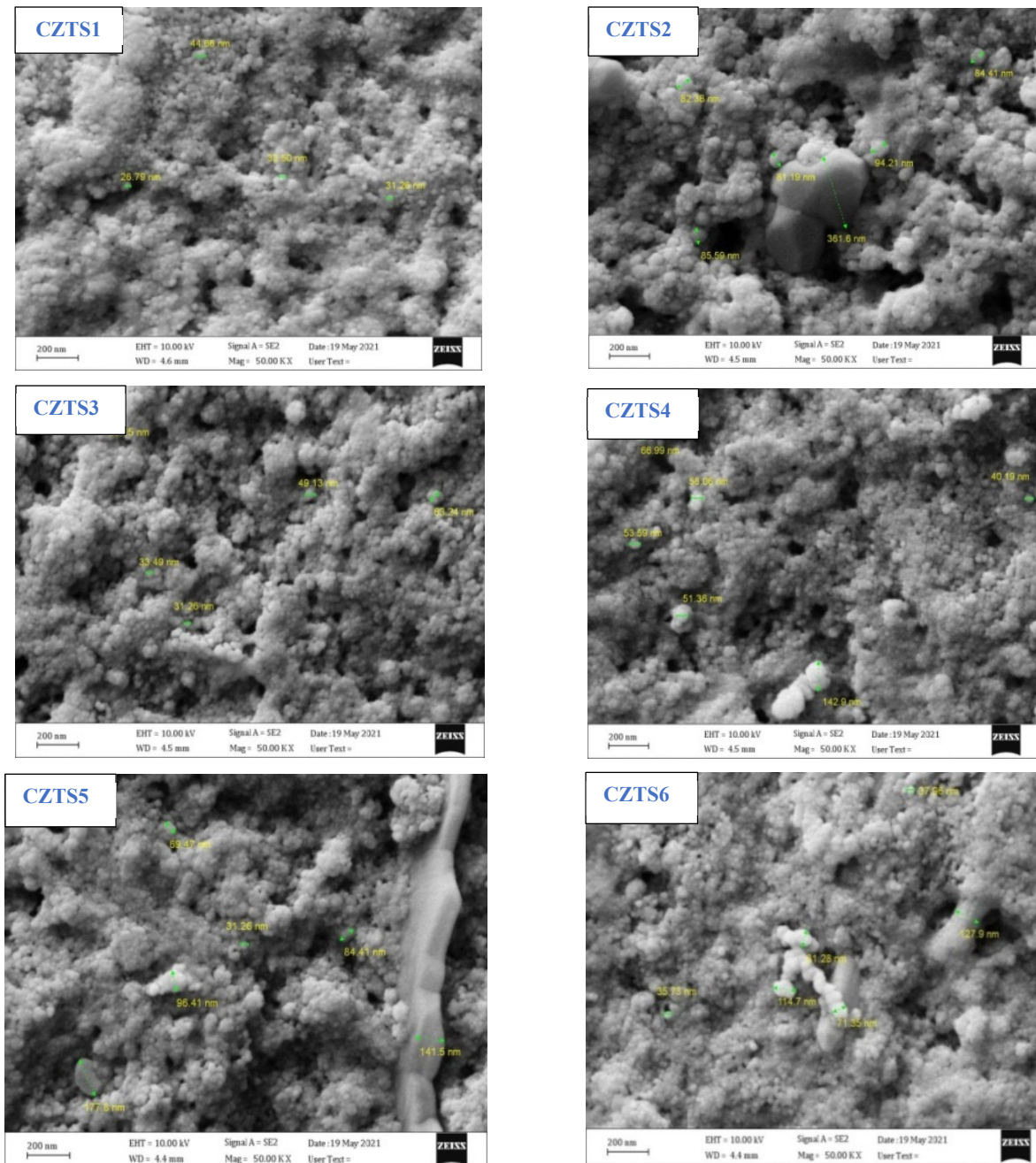


Figure 3. FESEM micro images of Na-doped CZTS thin films at different doping ratios

Optical measurements

The thin films optical absorption spectra were measured in the wavelength range of (300-900) nm using a UV-visible spectrophotometer. The investigation of the absorption coefficient based on photon energy is performed in the regions of high absorption to acquire thorough information about the energy band gaps of the films [18], and the absorption coefficient (α) is computed from the following equation [19]:

$$\alpha = 2.303A/t, \tag{4}$$

where (t) represents the thickness of the films and (A) is the absorbance.

The optical energy gap (E_g) of direct electronic transitions in films can be estimated from the absorbance spectrum using the equation:

$$\alpha h\nu = P(h\nu - E_g)^r, \quad (5)$$

where (P) is a constant dependent on the nature of the material, ($h\nu$) is the photon energy in (eV) units, E_g is the optical energy gap, and (r) is an exponential coefficient based on the transition nature ($r=2$ for allowed direct transition).

A graph is plotted between $(h\nu)^2$ and the incident photons energy ($h\nu$) (Tauc's plot) as represented in Figure 4. The energy gap value is estimated from intersection at the photon energy axis at the point $(\alpha h\nu)^2=0$. It can be noticed that the energy gap value of CZTS thin films decreases by increasing the Na-doping ratio. The energy gap values are 1.6, 1.58, 1.57, 1.53, 1.53 and 1.51 eV for the films CZTS1, CZTS2, CZTS3, CZTS4, CZTS5 and CZTS6 respectively.

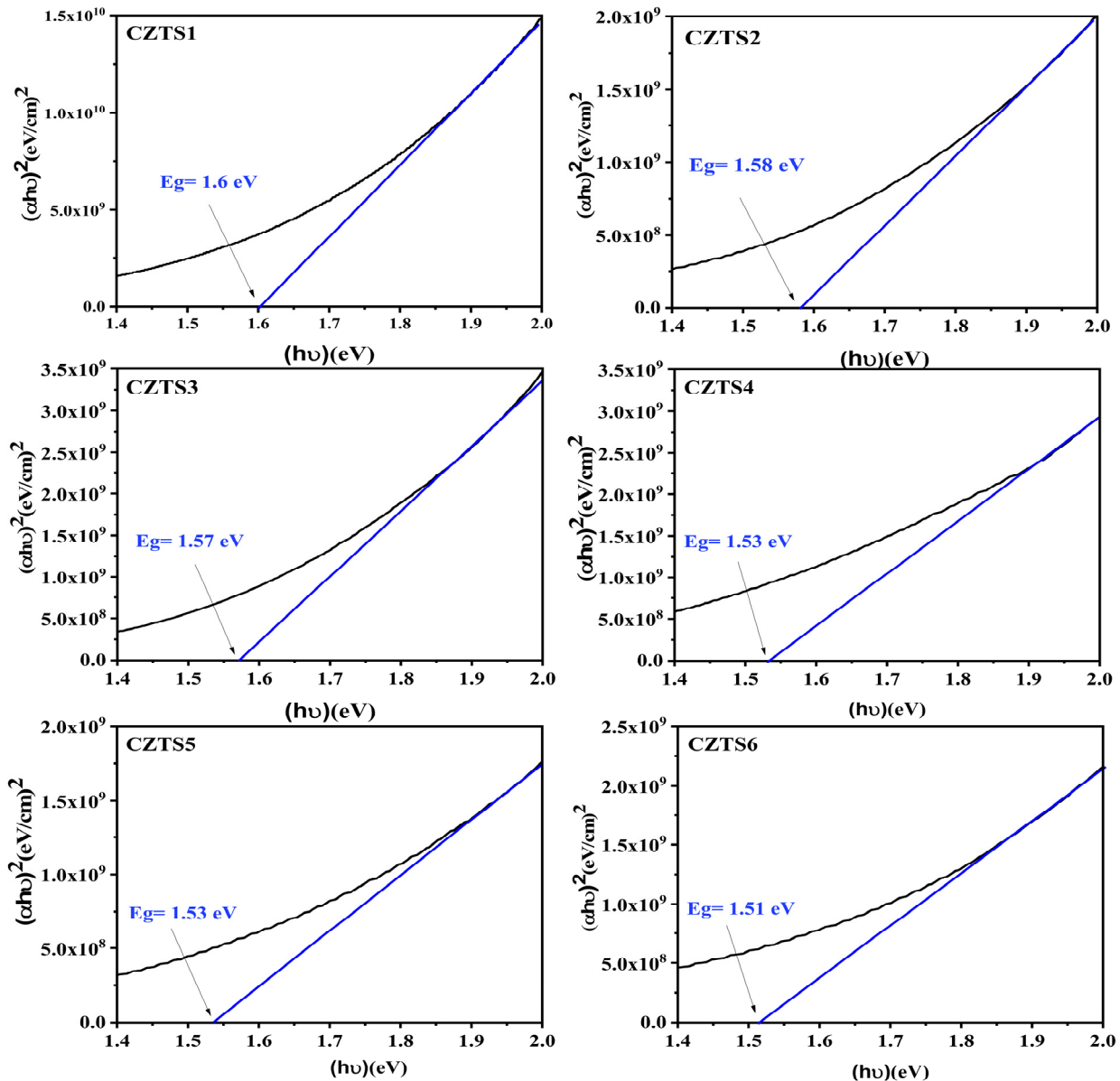


Figure 4. Tauc's plots of Na-doped CZTS thin films at different doping ratios.

The defects caused by Na are responsible for the reduction in band gap. When sodium is doped into a crystal, lattice distortion is induced leading to a change in the band gap. The substantial band gap decrease leads to the conclusion that the Na-doping model in the CZTS compound is an interstitial dopant, as it is the only model that combines band gap decrease and size reduction [20]. As a result, sodium acts to passivate defects in grain boundaries [21].

Electrical measurements

The Hall effect experiment was performed at room temperature to study electrical properties and specify the type, mobility and concentration of the majority charge carriers. According to Hall effect studies, the CZTS films have P-type conductivity, mobility of $\sim 8.07 \text{ cm}^2/\text{V}\cdot\text{s}$, and a maximum conductivity of $\sim 1.81 (\Omega\cdot\text{cm})^{-1}$, which corresponds to the films

CZTS6 as shown in Table 4. Figure 5 shows the variation of Hall conductivity with the Na doping ratio of CZTS thin films. Figure 6 shows the variation of the concentration and Hall mobility of the charge carriers as a function of Na doping ratio. From the two figures it can be concluded that the Na doping has improved the electrical properties of the deposited CZTS films.

Table 4. Results of the Hall effect experiment of Na-doped CZTS thin films at different doping ratios.

Sample	R_H (cm^3/C)	n (cm^{-3}) $\times 10^{18}$	μ ($\text{cm}^2/\text{V}\cdot\text{s}$)	ρ ($\Omega\cdot\text{cm}$)	σ ($\Omega\cdot\text{cm}$) $^{-1}$
CZTS1	7.3724	0.8466	4.5521	1.6196	0.6174
CZTS2	7.0213	0.8889	5.4251	1.2936	0.7730
CZTS3	6.1636	1.013	6.1331	1.0046	0.9954
CZTS4	5.5114	1.132	7.8556	0.7019	1.4247
CZTS5	4.4735	1.395	8.043	0.5563	1.7975
CZTS6	4.4627	1.399	8.0711	0.5528	1.8089

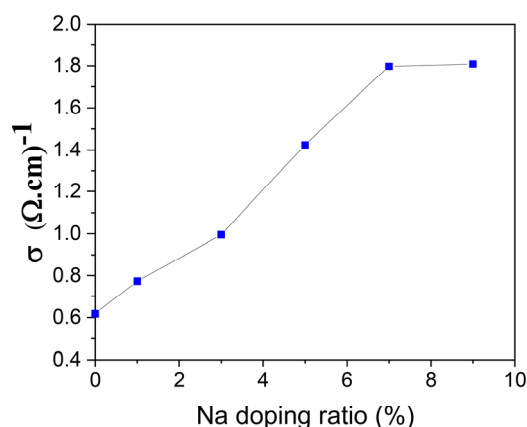


Figure 5. Variation of Hall conductivity of Na-doped CZTS thin films at different doping ratios.

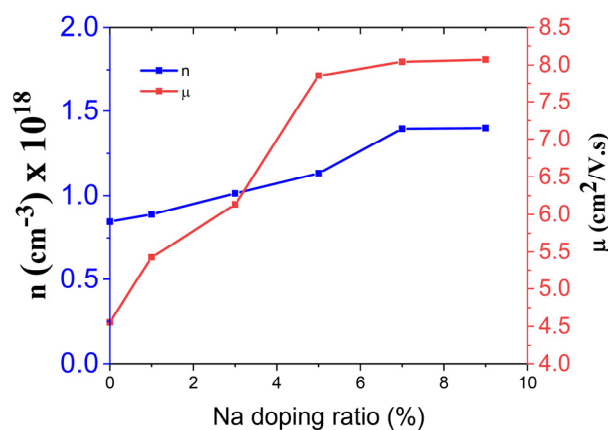


Figure 6. Variation of the concentration and Hall mobility of the charge carriers of Na-doped CZTS thin films at different doping ratios.

CONCLUSIONS

Na-doped CZTS thin films have been deposited successfully on glass substrates by chemical spray pyrolysis technique. The XRD experimental investigation of the films shows that they have kesterite tetragonal structure in the (112) favored direction. The crystallite size of all films was estimated using Scherrer's method, and it was found that the crystallite size decreases as the doping ratio increases. With increasing the Na volumetric doping ratio from 1 to 9 %, the optical band gap value decreases from 1.6 to 1.51 eV. Raman spectra of the films revealed a strong peak at $\sim 337 \text{ cm}^{-1}$ indicating the formation of the kesterite phase. On the other hand, all other observed low intensity peaks belong to the same phase confirming the absence of secondary phases. The FESEM surface morphology of the prepared Na-doped CZTS films was found to have cauliflower-like shapes in the nano-scale, with irregular particle size and distribution. Hall effect experiment on Na-doped CZTS films revealed that they have a P-type electrical conductivity with a low concentration of free holes. This test shows that the Na doping has improved the electrical properties of the deposited CZTS films.

ORCID IDs

✉ Noura J. Mahdi, <https://orcid.org/0000-0002-1219-0572>; ✉ Nabeel A. Bakr, <https://orcid.org/0000-0002-8819-5847>

REFERENCES

- [1] A. Polman, M. Knight, E.C. Garnett, B. Ehrler, and W.C. Sinke, "Photovoltaic materials: Present efficiencies and future challenges," *Science*, **352**(6283), aad4424 (2016). <https://doi.org/10.1126/science.aad4424>
- [2] P. Jackson, R. Wuerz, D. Hariskos, E. Lotter, W. Witte, and M. Powalla, "Effects of heavy alkali elements in Cu(In,Ga)Se₂ solar cells with efficiencies up to 22.6%," *Phys. Status Solidi*, **10**(8), 583 (2016). <https://doi.org/10.1002/pssr.201600199>
- [3] M.M.I. Sapeli, M.T. Ferdaous, S.A. Shahahmadi, K. Sopian, P. Chelvanathan, and N. Amin, "Effects of Cr doping in the structural and optoelectronic properties of Cu₂ZnSnS₄ (CZTS) thin film by magnetron co-sputtering," *Materials Letters*, **221**, 22 (2018). <https://doi.org/10.1016/j.matlet.2018.03.056>
- [4] K.I. Nakazawa, "Electrical and optical properties of stannite-type quaternary semiconductor thin films", *Japanese Journal of Applied Physics*, **27**(11), 2094 (1988). <https://doi.org/10.1143/JJAP.27.2094>
- [5] H. Katagiri, K. Jimbo, W.S. Maw, K. Oishi, M. Yamazaki, H. Araki, and A. Takeuchi, "Development of CZTS-based thin film solar cells", *Thin Solid Films*, **517**(7), 2455 (2009). <https://doi.org/10.1016/j.tsf.2008.11.002>
- [6] M. Buffiere, D.S. Dhawale, and F. El-Mellouhi, "Chalcogenide materials and derivatives for photovoltaic applications", *Energy Technology*, **7**(11), 1900819 (2019). <https://doi.org/10.1002/ente.201900819>

- [7] S. Giraldo, Z. Jehl, M. Placidi, V. Izquierdo-Roca, A. Pérez- Rodríguez, and E. Saucedo, "Progress and perspectives of thin film kesterite photovoltaic technology: a critical review", *Advanced Materials*, **31**(16), 1806692 (2019). <https://doi.org/10.1002/adma.201806692>
- [8] P.S. Patil, "Versatility of chemical spray pyrolysis technique", *Mater. Chem. Phys.* **59**(3), 185 (1999). [https://doi.org/10.1016/S0254-0584\(99\)00049-8](https://doi.org/10.1016/S0254-0584(99)00049-8)
- [9] N. Nakayama, and K. Ito, "Sprayed films of stannite $\text{Cu}_2\text{ZnSnS}_4$ ", *Applied Surface Science*, **92**, 171 (1996). [https://doi.org/10.1016/0169-4332\(95\)00225-1](https://doi.org/10.1016/0169-4332(95)00225-1)
- [10] Z. Laghfour, S. Aazou, M. Taibi, G. Schmerber, A. Ulyashin, A. Dinia, and Z. Sekkat, "Sodium doping mechanism on sol-gel processed kesterite $\text{Cu}_2\text{ZnSnS}_4$ thin films", *Superlattices and Microstructures*, **120**, 747 (2018). <https://doi.org/10.1016/j.spmi.2018.05.018>
- [11] Z. Tong, F. Liu, L. Jiang, and Y. Lai, "Improving the crystallization and carrier recombination of $\text{Cu}_2\text{ZnSnS}_4$ thin film deposited on Mo-coated soda-lime glass by extra sodium doping through solution process". *Materials Letters*, **254**, 50 (2019). <https://doi.org/10.1016/j.matlet.2019.07.014>
- [12] M. Marzougi, M.B. Rabeh, and M. Kanzari, "Effect of Na Doping on Structural and Optical Properties in $\text{Cu}_2\text{ZnSnS}_4$ Thin Films Synthesized by Thermal Evaporation Method", *Thin Solid Films*, **672**, 41 (2019). <https://doi.org/10.1016/j.tsf.2018.12.046>
- [13] C. Kittel, *Introduction to Solid State Physics*, (John Wiley and Sons Inc. 8th Edition, (2005).
- [14] B.D. Cullity, *Elements of X-ray Diffraction*, (Addison-Wesley publishing company, 1956).
- [15] E.M. Mkawi, "Kesterite $\text{Cu}_2\text{ZnSnS}_4$ Thin Films Synthesized Utilizing Electrodeposition: Influence of Metal Doping on the Properties", *International Journal of Energy Research*, **45**(2), 1908 (2021). <https://doi.org/10.1002/er.5873>
- [16] N.A. Bakr, S.A. Salman, and S.A. Hameed, "Deposition and Characterization of $\text{Cu}_2\text{ZnSnS}_4$ Thin Films for Solar Cell Applications", *International Journal of Applied Engineering Research*, **13**(6), 3379 (2018). https://www.ripublication.com/ijaer18/ijaerv13n6_32.pdf
- [17] D. Porezag, and M.R. Pederson, "Infrared Intensities and Raman-scattering Activities within Density-Functional Theory", *Physical Review B*, **54**(11), 7830 (1996). <https://doi.org/10.1103/PhysRevB.54.7830>
- [18] N.A. Bakr, Z.T. Khodair, and S.M. Abdul Hassan, "Effect of Substrate Temperature on Structural and Optical Properties of $\text{Cu}_2\text{ZnSnS}_4$ (CZTS) Films Prepared by Chemical Spray Pyrolysis Method", *Research Journal of Chemical Sciences*, **5**(10), 51 (2014). <http://surl.li/crxgq>
- [19] F. Zheng, X. Wen, T. Bu, S. Chen, J. Yang, W. Chen, F. Huang, and B. Jia, "Slow Response of Carriers Dynamics in Perovskite Interface upon illumination", *ACS Applied Materials and Interfaces*, **10**(37), 31452 (2018). <https://doi.org/10.1021/acsami.8b13932>
- [20] Z.K. Yuan, S. Chen, Y. Xie, J.S. Park, H. Xiang, X.G. Gong, and S.H. Wei, "Na-Diffusion Enhanced p-type Conductivity in $\text{Cu}(\text{In,Ga})\text{Se}_2$: A New Mechanism for Efficient Doping in Semiconductors", *Advanced Energy Materials*, **6**(24), 1601191 (2016). <https://doi.org/10.1002/aenm.201601191>
- [21] C.Y. Liu, Z.M. Li, H.Y. Gu, S.Y. Chen, H. Xiang, and X.-G. Gong, "Sodium Passivation of the Grain Boundaries in CuInSe_2 and $\text{Cu}_2\text{ZnSnS}_4$ for High-Efficiency Solar Cells", *Advanced Energy Mater.*, **7**(8), 1601457 (2017). <https://doi.org/10.1002/aenm.201601457>

ВПЛИВ ЛЕГУВАННЯ Na НА ДЕЯКІ ФІЗИЧНІ ВЛАСТИВОСТІ ТОНКИХ ПЛІВОК CZTS З ХІМІЧНИМ НАПИЛЕННЯМ

Ноура Дж. Махди, Набіль А. Бакр

Факультет фізики, Науковий коледж, Університет Діяла, Діяла, Ірак

У цій роботі тонкі плівки сульфиду міді-цинку-олова (CZTS), леговані натрієм, отримують шляхом нанесення їх на скляні підкладки при температурі (400 ± 10) °C і товщині (350 ± 10) нм за допомогою хімічного розпилювального піролізу (CSP). техніка. Як джерело використовували 0,02 М дигідрату хлориду міді ($\text{CuCl}_2 \cdot 2\text{H}_2\text{O}$), 0,01 М хлориду цинку (ZnCl_2), 0,01 М дигідрату хлориду олова ($\text{SnCl}_2 \cdot 2\text{H}_2\text{O}$), 0,16 М тіосечовини ($\text{SC}(\text{NH}_2)_2$). іони міді, цинку, олова та сірки відповідно. Як джерело легуючої домішки використовувався хлорид натрію (NaCl) у різних об'ємних співвідношеннях (1, 3, 5, 7 та 9) %. Розчин напилюють на скляні підкладки. Для дослідження структурних, оптичних та електричних властивостей отриманих плівок використовувалися методи XRD-дифракції, рамановської спектроскопії, FESEM, UV-Vis-NIR та методу ефекту Холла. Результати дифракції XRD показали, що всі плівки є полікристалічними, з тетрагональною структурою та переважною орієнтацією вздовж площини (112). Розмір кристалітів усіх плівок було оцінено за допомогою методу Шеррера, і було виявлено, що розмір кристалітів зменшується зі збільшенням коефіцієнта легування. Результати FESEM показали існування наночастинок у формі цвітної капусти. Показано, що ширина забороненої зони оптичної енергії становить від 1,6 до 1,51 eV з високим коефіцієнтом поглинання ($\alpha \geq 10^4$ см⁻¹) у видимій області спектра. Вимірювання Холла показали, що провідність тонких плівок CZTS з різними коефіцієнтами легування Na має електропровідність р-типу, і вона зростає зі збільшенням коефіцієнта легування Na.

Ключові слова: тонкі плівки CZTS, легування натрієм, структурні властивості, оптичні властивості, ефект Холла.